Interaction mechanism of N_2 with the Cr (110) surface

T. C. Guimarães* and A. C. Pavão
Departamento de Química Fundamental, Universidade Federal de Pernambuco 50.670-900, Recife, Pernambuco, Brazil

C. A. Taft
Centro Brasileiro de Pesquisas Fisicas, Rua Xavier Sigaud 150, 22290-180, Rio de Janeiro, Rio de Janeiro, Brazil

W. A. Lester, Jr.
Chemical Sciences Division, Lawrence Berkeley National Laboratory and Department of Chemistry, University of California, Berkeley, California 94720-1460

(Received 23 October 1996)

The interaction of N_2 with the Cr (110) surface is analyzed using the *ab initio* Hartree-Fock method and a Cr_5N_2 cluster. Our results indicate that the tilted state is energetically favored over perpendicular adsorption. The Mulliken surface→N_2 charge transfer, overlap populations as well as N-N distances increase in the tilted configuration. We also analyze the stretching frequencies, geometrical parameters, natural bond orbital populations, density of states, orbital energies, charge-density distribution and orbital contours. We propose a model to explain the catalytic dissociation of N_2 on the Cr (110) surface. [S0163-1829(97)05135-7]

I. INTRODUCTION

The reaction of nitrogen with transition-metal surfaces is of considerable theoretical and technological importance. It has practical importance in the preparation of nitride coatings, the stability of ceramic-metal interfaces, and plays an important role in understanding the processes of heterogeneously catalyzed ammonia synthesis. Although the dissociation of N_2 is an important phase in determining the rate of synthesis of ammonia using iron as a catalyst, the mechanism is still not well understood. A correct characterization of the molecular states involved in the mechanism of dissociation of a molecule on a metal surface may facilitate future progress in the field of heterogeneous catalysis.

A comparison of nitrogen molecule chemisorption and dissociation with that of isoelectronic carbon monoxide[1–5] may provide useful information on how N_2 interacts with metal surfaces, assuming different bonding geometries, strengths, and electronic configurations.[6–8] It is well known that CO is adsorbed with the carbon atom closest to the surface. On most densely packed metal surfaces CO is adsorbed with the molecular axis parallel to the surface normal. On the Fe (100) and Cr (110) surfaces, however, a CO tilted molecular state is also observed.[6] *Ab initio* Hartree-Fock (HF) self-consistent-field calculations predict that the tilted state may occur on all the dissociative surfaces.[2] In the linear metal-CO complex, the interaction is described by the Blyholder model[5] in which the bond is formed by electron transfer from the $5s$ orbital of CO to unoccupied metal orbitals, accompanied by back donation of electrons from occupied d orbitals into the unoccupied 2π orbitals of CO. A similar picture can be used to describe the bonding of the metal with N_2. For the nitrogen molecule, the molecular orbitals that participate predominantly in bonding to the surface are the donating orbitals $3\sigma_g$ and $2\sigma_u$ that are essentially nonbonding with respect to the molecular bond (the N_2 $3\sigma_g$ orbitals are weakly bonding and the N_2 $1\pi_g$ are strongly antibonding).[9]

Both experimental and theoretical[8,10–22] studies have shown that N_2 is weakly chemisorbed via one nitrogen atom and oriented with its intramolecular axis nearly perpendicular to most transition-metal surfaces, such as Ni,[8,10,11,19–21] Pd,[8] Ru,[12,17] W,[13,23] Re,[15] and Ir.[16] The perpendicular geometry is also described by the Blyholder model.[5] However, other experiments have shown that N_2 is strongly chemisorbed on Fe (111),[24–26] Cr (111),[27] and Cr (110) (Ref. 28) with its intramolecular axis parallel to the surfaces, i.e., as π-bonded N_2.[25]

The adsorption of diatomic molecules such as CO and N_2 on metal surfaces has been extensively studied by core valence photoemission.[29] Despite considerable knowledge of diatomic-metal interactions, however, there are still unanswered questions regarding the assignment of the observed spectra, including the origin of strong satellite lines observed for several transition-metal surfaces. Whereas, photoelectron spectroscopy mainly probes the electronic properties of adsorbates, vibrational spectroscopy[30] has also provided rich information on bonding sites, geometries, and underlying electronic properties. In weakly chemisorbed systems[8,10,31,32] such as CO/Cu and N_2/Ni there has been controversy[33] in identifying the nature of the valence electron spectra. Heskett, Plummer, and Messmer[34] observed that the appearance of satellite lines due to multielectron excitation in the weakly chemisorbed systems mentioned above is always accompanied by an unusual shift of the molecular vibrational frequencies dependent on the molecular coverage. The vibrational frequencies decrease with increasing coverage in contrast to the predictions of dipole-dipole coupling theory.[35] It is proposed that these properties can be qualitatively understood as a consequence of the lack of $2\pi^*$-metal bonding in the ground state. Instead of $2\pi^*$-metal bonding, the $5s$ orbital would be responsible for the bond to the substrate leading to a decrease of the C-O stretching frequency as molecular cov-

erage increases. Experiments also indicate a negative shift and substantial broadening of the vibrational spectra of these molecules that is dependent upon the strength of chemisorption on the metal surfaces. Ueba[7] proposed a unified theory which enables us to understand the electronic and vibrational properties in terms of the occupancy of the low-lying $2\pi^*$ level in the neutral ground state and in the vibrational excited state of chemisorbed molecules. Also discussed are the changes of vibrational frequencies with coverage due to charge transfer between the $2\pi^*$ level and the metal.

Adsorption of molecular nitrogen and its subsequent dissociation into atomic nitrogen on Fe (111) has been studied in some detail.[36,37] Two weakly chemisorbed molecular N_2 states have been identified mainly via high-resolution electron-energy-loss spectroscopy (HREELS) and thermal-desorption spectroscopy.[25,38] In the so-called γ state, with an adsorption enthalpy of ~ 0.25 eV,[26] the N_2 molecules are terminally bonded to first-layer Fe atoms.[39] The slightly stronger bound α state, with an adsorption enthalpy of ~ 0.32 eV,[26] which is the precursor to N_2 dissociation on the surface, has been attributed to N_2 π-bonded to the surface.[25] While the γ state has recently been found to have a vibrational N-N stretching frequency of 2100 cm^{-1},[39] the α state exhibits an unusually low stretching frequency of 1490 cm^{-1}, which in turn was used to infer, together with x-ray photoemission spectroscopy (XPS) results, a π-bonded state.[25] According to theory and experiments, α and γ states are separated by an activation barrier that has been determined experimentally to be approximately 0.21 eV.[26] The separation of α and γ states by an activation barrier allows one to depopulate selectively the γ state at higher temperature (above 110 K), while at lower temperature (below 77 K) α and γ states are both populated.[39] Angle-resolved photoelectron spectra excited by synchrotron radiation were obtained for adsorbed N_2 on Fe (111) as a function of temperature by Freund *et al.*[26] which indicated that the two previously identified phases of molecular N_2, i.e., the γ and α phases, can be clearly differentiated by their photoemission characteristics. The γ phase can be shown to consist of N_2 molecules oriented perpendicular to the surface plane whereas the α-phase spectrum is only consistent with the N_2 axis inclined from the surface normal. These findings are in agreement with HREELS and XPS experiments that N_2 in the α phase is ''π-bonded'' to the surface. *Ab initio* generalized valence-bond calculations of the excited state of N_2 suggested that this state may be stabilized by the Fe (111) surface resulting in the species responsible for the α phase—a ''π-bonding'' state.

Dowben *et al.*[40] investigated dissociative adsorption of N_2 on Cr (110) and Fe_7Cr_{28} (110) and reported that small concentrations of elemental iron at the surface reduces the probability of dissociative nitrogen adsorption. Since geometrical arguments, based on the distribution of chromium clusters of sufficient size to dissociate an N_2 molecule, cannot explain the decrease in dissociation probability, these authors have concluded that the presence of iron decreases the chemical activity of Cr for breaking the N_2 bond via electronic structure effects. Dowben, Ruppender, and Grunze[41] investigated the adsorption of nitrogen molecule on Cr (110) at 100 K and found strong evidence to support the existence of a weakly bound molecular state with a heat of desorption of ~ 0.15 eV.

Some of the recent work has focused on various aspects of adsorbates, substrates, and their interactions. These include cluster models of the energy of vacancy formation in metals,[42] electronic structure of atomic adsorbates from x-ray absorption spectroscopy, threshold effects and higher excited states,[43] autonization as a tool for interpretation of x-ray absorption spectra,[44] critical size for a metal-nonmetal transition in transition-metal clusters,[45] surface relaxation of transition-metal surfaces with a nearly filled *d* band,[46] one-dimensional image state on stepped transition metals,[47] vibrational and orientation factors in selective probing of intramolecular potentials in physisorbed molecules,[48] and higher excited states in x-ray absorption spectra of adsorbates.[49]

In this work, we investigate the perpendicular (γ) and the tilted (α) states, with freedom of orientation, of N_2 adsorption on the Cr (110) surface. To represent the surface we consider a model formed of five Cr atoms. We investigate charge transfer, interatomic distances, binding energies, activation energies, stretching frequencies, Fermi levels, back donation, densities of states, and orbital eigenvalues. Pauling's theory of nonsynchronized resonance[1–5,50] is used to analyze the catalytic mechanism of N_2 dissociation on the Cr (110) surface. Based on the resonating valence bond theory, the present study presents a consistent description of the molecular states involved in the interaction which correlates well with experiments. The mechanism is based on resonant states of chemical bonds involving atoms of the molecule and the surface. There is a two-stage electron transfer to and from the surface involving an intermediate predissociative state with large charge transfer in which the molecule is inclined with respect to the surface. With an adequate comprehension of the molecular states it may be possible to test new catalytic surfaces where the molecules are positioned in ori-

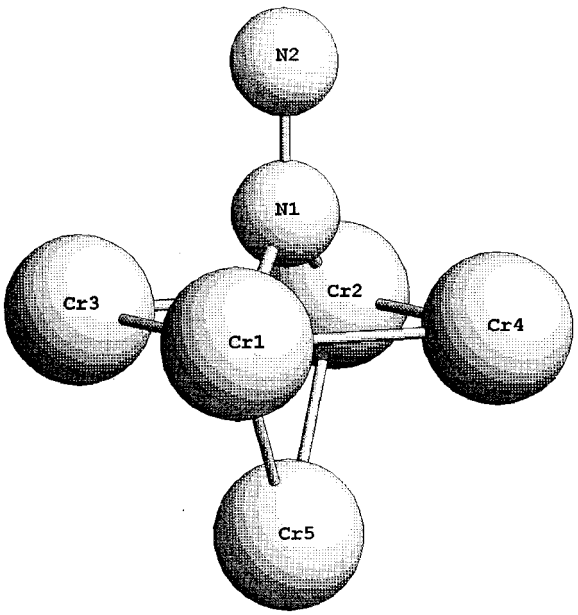

FIG. 1. Perpendicular configuration of N_2 adsorption on Cr_5N_2 cluster model representation of the Cr (110) surface.

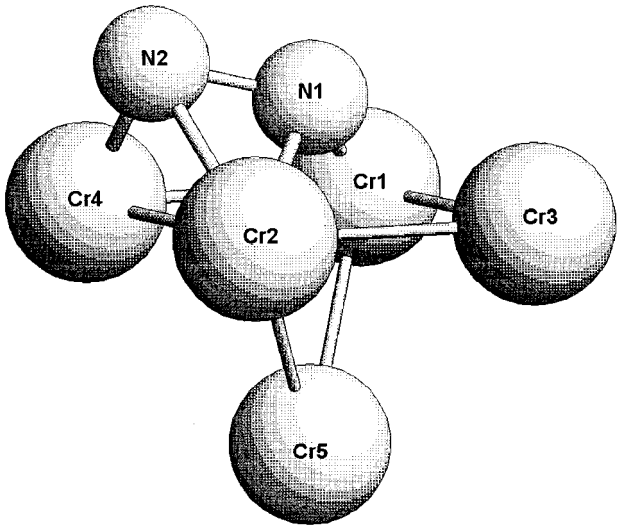

FIG. 2. Near parallel configuration of N_2 adsorption on Cr_5N_2 cluster model representation of the Cr (110) surface.

entations that permit greater efficiency in the dissociation process.

II. COMPUTATIONAL DETAILS

The calculations were carried out with GAUSSIAN 92[51] using the restricted HF method with effective core potentials and the basis sets of Hay and Wadt.[52] The Cr (110) surface was described by five Cr atoms (Figs. 1 and 2). The Cr (110) surface geometry was fixed at the experimental bulk values whereas the adsorbed or dissociated N_2 geometry was optimized to yield interatomic distances, angles, and dihedral angles. In addition to Mulliken population analysis, a natural bond orbital population (NBO) analysis[53] has been used to determine charges and orbital population of the Cr_5N_2 cluster. The NBO is an alternative to conventional Mulliken population analysis[54] that provides an improved electron distribution.

There are serious limitations to the cluster quantum chemical method. These shortcomings include the imposed boundary conditions, the charge accumulated in the tiny metal cluster, and the extreme discretization of energy states in the cluster. However, the purpose here is to compare the charge transfer between the adsorbed molecule and the metallic surface for different geometries. In such a comparative analysis, the finite-size effects [five Cr atoms to represent the (110) surface] are expected to be minimal. We base this view in part on our earlier work[1–4] using smaller clusters for other transition-metal surfaces with adsorbed diatomic molecules. In that work a comparative analysis among various geometries of the calculated charge transfer yielded reasonable results also in agreement with experiment.

In Tables I–V we give results at the stationary points of the full geometry optimization of the Cr_5N_2 cluster which is used to model the adsorption of N_2 on the Cr (110) surface. (A frozen core description for N_2 is used throughout.) In these tables we give information regarding the configuration with N_2 perpendicular to the surface and N_2 inclined nearly parallel to the surface. For each adsorption geometry (Figs. 1 and 2, Table I) we give the bond length R(N-N); the adsorption height R(N-surface), which is the perpendicular distance from the surface (Fig. 1) to the first nitrogen (N1), the distance between Cr1 and the projection of N1 on the Cr1-Cr2 axis R(Cri-Pr(N)), as well as the angle between the N-N bond axis and the surface determined by atoms (Cr1, Cr2, Cr3, Cr4), and the clockwise rotation angle of the nearly parallel N_2 bond axis from the short axis toward the long-axis direction. In Table II we give the Mulliken[54] overlap populations and charge transfer from the surface, the N_2 stretching frequency calculated at the fully optimized geometry, as well as the binding energy corresponding to the geometries given in Table I.

In this and subsequent sections we analyze the effect of tilting the N-N axis on the interatomic distances, Mulliken overlap populations, charge transfer, and stretching frequencies. The adsorption geometry (Fig. 2) at the fourfold site with the N-N axis nearly parallel to the surface forming an angle of 14.2° with respect to the surface (with a small shift 0.04 Å along the short axis) from the center of the plane (formed by Cr1, Cr2, Cr3, Cr4), was the most stable geometry (lowest total energy) with a binding energy about three times larger than that calculated at the fourfold vertical position (Table II). The inclination of the vertical position, until an angle of 14.2° with respect to the surface is attained, results in increased charge transfer ($0.47 \rightarrow 0.79$) from the surface to N_2, an increase of R(N-N) ($1.34 \rightarrow 1.43$ Å), reduction of the R(surf-N) surface-nitrogen distance ($1.07 \rightarrow 1.00$ Å), and increase of Mulliken overlap population ($0.244 \rightarrow 0.299$) as we go from the perpendicular to the nearly parallel configuration. A reduction of the N1-surface interaction distance with corresponding increase of N—N

TABLE I. Optimized geometry for the Cr_5N_2 cluster representation of the Cr (110) surface.

Geometry[a]	N_2 orientation	R(N-N)[b] (Å)	R(surf-N)[c]	R(Cri-Pr(N))[d]	(e)	(f)
g	Near parallel	1.428	0.996	1.482	14.18	59.08
h	Perpendicular	1.343	1.066	1.440	90.0	0.0

[a]Optimized geometry maintaining fixed C-Cr experimental interatomic distances.

[b,c,d]R(N-N), R(surf-N), R(Cri-Pr(N)), $i=1,2$, indicates molecular nitrogen interatomic distances (angstroms), perpendicular height of N above surface, and the distances between Cri ($i=1$) and the projection of N on the Cr1-Cr2 axis.

[e]Angle (degrees) between N_2 bond axis and the surface.

[f]Clockwise rotation angle (degrees) of nearly parallel N_2 bond axis from short axis towards long-axis direction.

[g]Near parallel indicates N_2 with nearly parallel inclination to surface along short axis.

[h]Perpendicular indicates N_2 perpendicular to surface.

TABLE II. Mulliken overlap population, surface→N_2 charge transfer and N_2 stretching frequencies for Cr_5N_2 cluster representation of the Cr (110) surface.

Geometry[a]	N_2 orientation	Overlap population[b]	Charge transfer[c]	N_2 stretch frequency[d]	Binding energy (eV)
e	Near parallel	0.244	−0.79	1220 (2359)[f] [2670][g]	5.44
h	Perpendicular	0.299	−0.47		1.74

[a]Optimized geometries described in Table I.
[b]Mulliken N1-N2 overlap population.
[c]Mulliken surface→N_2 charge transfer.
[d]N_2 stretching frequency in cm^{-1} (frequency determined in fully optimized near parallel configuration).
[e]N_2 with near parallel inclination to surface along short axis.
[f]Experimental free gaseous N_2 stretching frequency.
[g]Our calculated free N_2 stretching frequency.
[h]N_2 perpendicular to surface.

bond length indicates that the N1-surface bond was strengthened whereas the molecular N—N bond was weakened. The stretching frequency of 1220 cm^{-1}, calculated at the fully optimized geometry, is small (estimated 50% reduction) compared to the stretching frequencies corresponding to adsorption of molecular N_2 on Ni (100), Ru (100), and W (100) surfaces,[8,14,17] which are on the order of 2200–2330 cm^{-1} (closer than that of the experimental free nitrogen molecule 2359 cm^{-1}) suggesting, according to our previous model,[1–4] nondissociative Ni, Ru, and W surfaces as opposed to a dissociative Cr (110) surface. The small stretching frequency calculated for N_2 adsorption on the chromium surface can be correlated with weakening of the N—N bond. Stretching frequencies of approximately 1100 cm^{-1} have been observed in transition-metal compounds containing nitrogen with bond order of 1. The N—N bond length of 1.42 Å calculated in the nearly parallel configuration is characteristic of a single bond.[54] Stretching frequencies of ~2400 cm^{-1} have been observed for nitrogen molecule with bond order larger than 1. We note that the experimental bond length of the free N-N molecule is approximately 1.098 Å, whereas, in transition-metal compounds we find this distance to be ~1.2 Å for N═N and larger (~1.3 Å) for N—N. Our calculated bond distance for the free nitrogen molecule is 1.139 Å and corresponding stretching frequency is 2670 cm^{-1}.

In Table III we give the Mulliken and NBO atomic charge as well as Mulliken overlap population for the Cr_5N_2 cluster. In the perpendicular configuration N1 is closer to Cr1 and

TABLE III. Mulliken and natural bond orbital atomic charge and overlap population for Cr_5N_2 cluster.

N_2 orientation	Mulliken and NBO population						Mulliken overlap population			
	Cr1	Cr2	Cr3	Cr4	N1	N2	Cr1-N1 / Cr1-N2	Cr2-N1 / Cr2-N2	Cr3-N1 / Cr3-N2	Cr4-N1 / Cr4-N2
Nearly parallel orientation							0.36	0.16	0.05	−0.111
Mulliken population analysis	0.17	0.31	0.21	0.22	−0.48	−0.3	/ −0.08	/ 0.15	/ −0.02	/ 0.36
NBO 0.19	0.39	0.12	0.23	−0.62	−0.49					
Perpendicular geometry							0.22	0.19	0.02	0.02
Mulliken population analysis	0.16	0.16	0.11	0.11	−0.52	0.056	/ 0.01	/ 0.01	/ 0.00	/ 0.00
NBO	0.20	0.32	0.14	0.14	−0.69	0.02				

TABLE IV. Variation of Mulliken charges and overlap population with inclination.

Angle[a] (deg)	5	55	63	68	72	80	85
q(N1)	−0.51	−0.50	−0.50	−0.50	−0.49	−0.46	−0.46
q(N2)	0.05	−0.24	−0.28	−0.29	−0.30	−0.31	−0.31
q(Cr1)	0.11	0.17	0.16	0.17	0.17	0.17	0.17
q(Cr2)	0.23	0.20	0.25	0.27	0.30	0.33	0.34
q(Cr3)	0.13	0.22	0.22	0.22	0.22	0.20	0.19
q(Cr4)	0.18	0.20	0.24	0.24	0.23	0.21	0.19
Ov(N2-Cr4)	0.00	0.24	0.30	0.32	0.35	0.38	0.39
Ov(N2-Cr2)	0.00	0.15	0.16	0.16	0.15	0.15	0.14
Ov(N2-Cr1)	0.00	0.04	0.06	0.01	0.07	0.09	0.08

[a]Inclination angle with respect to surface normal; q an Ov indicate Mulliken atomic and overlap populations, respectively.

Cr2 and both the Cr1-N1 and Cr2-N1 separations are 1.72 Å. The latter species also have the same overlap (0.20) whereas N1 is more distant (2.24 and 2.99 Å) from the (Cr3, Cr4) and Cr5 atoms, respectively, with corresponding negligibly small (0.01) overlaps (Figs. 1 and 2). The overlap between N2 and the surface chromium atoms, in the perpendicular position, where N2 is at distances of 2.44 and 2.83 Å from the (Cr1, Cr2) and (Cr3,Cr4) atoms, respectively, is also negligibly small. When the nitrogen molecule inclines with an angle of 14.2° with respect to the surface there is a small reduction in the surface-N1 distance and a slight shift of N1 along the short axis. The largest changes in interatomic distances correspond to the N2-surface distance changes with inclination. The N2-Cr2 interatomic distance is reduced from 2.44 Å in the perpendicular configuration to 1.96 Å in the nearly parallel configuration. Similarly, the N2-Cr4 bond distance is substantially reduced from 2.83 to 1.71 Å. As opposed to Cr2 and Cr4, the Cr1-N2 and Cr3-N2 distances increase from 2.44 to 2.77 Å and 2.83 to 3.56 Å, respectively, which is not favorable for enhanced bonding interaction. The overlaps in the nearly parallel configuration between Cr4-N2 and between Cr2-N2 are 0.36 and 0.15, respectively, increasing in the same order as their respective bond lengths. As expected, with larger interatomic distances in the parallel configuration the Cr1-N2 and Cr3-N2 Mulliken overlap populations are negligibly small. We note that the largest Mulliken overlap population of N2-Cr2 (0.36) has increased considerably from its value in the perpendicular configuration (0.01).

In the following sections we analyze and compare in more detail the Mulliken and NBO atomic and orbital populations for the perpendicular, near parallel as well as the entire inclination process. In Table V we give the occupation of the NBO in the perpendicular and inclined (14.2 °) configurations. We first note that in the Cr_5N_2 perpendicular configuration, N_2, has 10.68 valence electrons, i.e., 0.68 electrons more than in the free N_2. In the inclined Cr_5N_2 configuration

TABLE V. Natural atomic orbital occupancies in near parallel and perpendicular configurations. Values in parentheses correspond to nearly perpendicular configuration. Values without parentheses correspond to nearly parallel configuration.

Orb	Cr1	Cr2	Cr3	Cr4	Cr5	N1	N2
$4s$	0.94	0.66	1.24	0.78	1.02		
	(0.95)	(0.82)	(1.22)	(1.23)	(1.51)		
dxy	0.70	1.04	1.06	1.10	.32		
	(0.23)	(1.95)	(0.55)	(0.49)	(0.10)		
dxz	1.57	0.96	0.52	0.68	0.91		
	(1.81)	(0.11)	(0.56)	(0.63)	(1.00)		
dyz	1.22	1.28	1.32	0.47	1.16		
	(0.50)	(0.73)	(1.17)	(0.98)	(0.49)		
dx^2-y^2	1.02	1.02	0.75	1.02	1.45		
	(1.69)	(0.35)	(1.36)	(1.45)	(1.82)		
dz^2	0.24	0.51	0.83	1.53	0.81		
	(0.52)	(1.59)	(0.91)	(0.95)	(1.15)		
$2s$						1.65	1.74
						(1.61)	(1.83)
px						1.20	1.02
						(1.42)	(0.29)
py						1.34	1.39
						(1.20)	(1.02)
pz						1.43	1.33
						(1.47)	(1.84)

N_2 has 11.10 electrons, i.e., 1.10 more electrons than free N_2. In the parallel configuration N_2 has 0.42 more electrons than in the perpendicular orientation. These NBO data show that there is a net charge transfer from the surface to the adsorbed nitrogen molecule, perhaps considerable back donation, which would be important for explaining the substantial weakening of N—N bond, and significant reduction of the stretching frequency.

We note from the NBO analysis (Table V) that the second nitrogen (N2) of the adsorbed nitrogen molecule (Fig. 2) has 4.98 valence electrons in the perpendicular orientation, 5.48 electrons in the inclined orientation and 5 electrons in the free nitrogen molecule. As expected from our previous analysis of Cr-N interatomic distances, in the near parallel configuration, the N2 atom, which is nearest to the surface chromium atoms Cr4 and Cr2, is apparently a stronger participant in bonding, back donation, and general charge-transfer effects with the surface Cr atoms. Analysis of the $\sigma(2s+2p_z)$ orbitals indicates that there are 6.75 electrons in the Cr_5N_2 perpendicular configuration and 6.15 electrons in the inclined configuration yielding a net σ donation of 0.60 from the vertical to the inclined (near parallel) orientation.

We observe from Table V that in the perpendicular orientation the nitrogen atom N1 (closest to the surface) has in its $\sigma(2s+2p_z)$ orbital approximately the same number of electrons (~ 3.0) found in the free nitrogen molecule. The negative N1 charge [NBO (-0.62), MK (-0.48), see Table III] may thus have its origin in other interactions, such as π interactions with the surface. Alternatively, in going from the perpendicular to the nearly parallel configuration, the occupation of the N2 $\sigma(2s+2p_z)$ orbital decreases from 3.67 to 3.07 whereas the occupation of the $\pi(2p_x+2p_y)$ orbitals increases from 1.31 to 2.41. In the inclined configurations the N2 atom (which is closer to the surface chromium atoms) becomes negatively charged. Table IV shows that as N_2 is inclined towards the surface chromium atoms, the N2 charge diminishes, becomes negative with inclination and stabilizes at ~ -0.31 as it gets close to the surface. During the inclination of N_2, the N1 atom (which is initially closest to the surface) does not change substantially, but becomes slightly more positive during the course of reaction. As the adsorbed N_2 is inclined, the chromium atoms whose charges are most affected are Cr4 and Cr2, in the same order as the reduction of interatomic distances. As previously discussed, the Cr3-N2, Cr1-N2 distances are larger and consequently the charges on Cr1 and Cr3 are not as affected with inclination, remaining at ~ 0.2. The Cr3-N2 and Cr1-N2 overlap remains essentially small or negligible during the entire inclination process to the parallel position. The Cr4 and Cr2 charges increase to ~ 0.35 for Cr2 ~ 0.21 for Cr4 with inclination to the parallel configuration. The Mulliken overlap population also increases substantially with approach to the parallel configuration becoming ~ 0.38 for Cr4-N2 overlap and ~ 0.15 for Cr2-N2 overlap. We note that beyond the transition barrier at $\sim 50°$ the large negative N2 charge (-0.23) and the large positive Cr charge (0.23) combined with a shorter Cr4-N2 distance with inclination, will introduce a substantial electrostatic interaction contribution which is coincident with a steep lowering of the energy and stabilization of the system.

Concentrating attention now only on the $2s$ orbitals of Tables III and IV we note that the NBO of N1 and N2 have a total occupancy of 3.44 electrons in the perpendicular configuration and 3.39 electrons in the inclined orientation which indicates a small donation of 0.05 electrons between the two configurations. The free N_2 has 3.46 electrons in the $2s$ orbital so that its participation in the interaction with the chromium surface appears to be negligibly small. The largest changes (0.45 and 0.16) in the Cr($4s$) orbital between perpendicular and parallel configurations occurs for Cr4 and for Cr2 which follows again the order of decreasing interatomic Cr-N distances. The total NBO $2p_z$ occupancy of N1 and N2 goes from 3.31 to 2.76 electrons in going from the perpendicular orientation to the inclined orientation indicating a donation of 0.55 electrons. Free N_2 has only 2.54 electrons in the $2p_z$ orbital, indicating that there is no $2p_z$ donation from free N_2 to the perpendicular or inclined configurations. The Cr($4p$) occupation is small in both perpendicular and parallel configurations (0.1–0.2).

The $\pi(p_x)$ and $\pi(p_y)$ orbitals of the adsorbed nitrogen molecule have 3.93 electrons in the perpendicular and 4.95 electrons in the near parallel configuration. The number of π electrons in the perpendicular configuration is closer to the number of electrons in free N_2 and indicates a large π donation (~ 1 electron) to the adsorbed N_2 in the parallel orientation, in these so-called π-bonded systems. The much larger back donation (increase of π antibonding orbital population) in the nearly parallel configuration would explain the weakening of the N—N bonds and the larger binding energies in this configuration. As the N2 atom inclines towards Cr2, Cr4, the strong interaction between the increasing negatively charged N2 atom and the positively charged Cr4 and Cr2 atoms of the surface favors the parallel configuration, lowering the total energy of the system.

In the following sections, we analyze the HOMO (highest occupied molecular orbital), LUMO (lowest unoccupied molecular orfbital), Fermi energy, composition of bonding orbitals, density of states, charge densities, and contour plots for the perpendicular and near-parallel configurations. In Fig. 3 we show the orbital energies for the bare cluster representation of the Cr (110) surface as well as the Cr_5N_2 cluster representation of the perpendicular and near-parallel configurations. Proceeding from the perpendicular to the near-parallel configuration there is a lowering of the orbital energy levels. In the near-parallel configuration the Fermi energy (HOMO) is lower than in the perpendicular configuration. The LUMO energy level in the parallel configuration is also lower than in the perpendicular configuration. Lowering of the Fermi and LUMO energies in the near-parallel configuration facilitates the occupation of the N_2 antibonding orbitals localized above the Fermi level and occupation of the bonding orbitals of the transition-metal surface, and weakening the N—N bond. In the parallel configuration the energy levels are more closely spaced and piled up at the Fermi level. Most of the orbitals have a mixture of both N and Cr components in both the parallel and perpendicular configurations. However, the mixing of N and Cr orbitals is larger in the parallel configuration.

The NBO bond orbital method also indicates, in the near-parallel configuration, Cr2-N2 and Cr4-N2 bonding which also correspond to the closest chromium-nitrogen interatomic distances. The Cr2-N2 bonding orbital is mostly N2 (4% s 96% p) with Cr (14% s, 8% p, 78% d) participation.

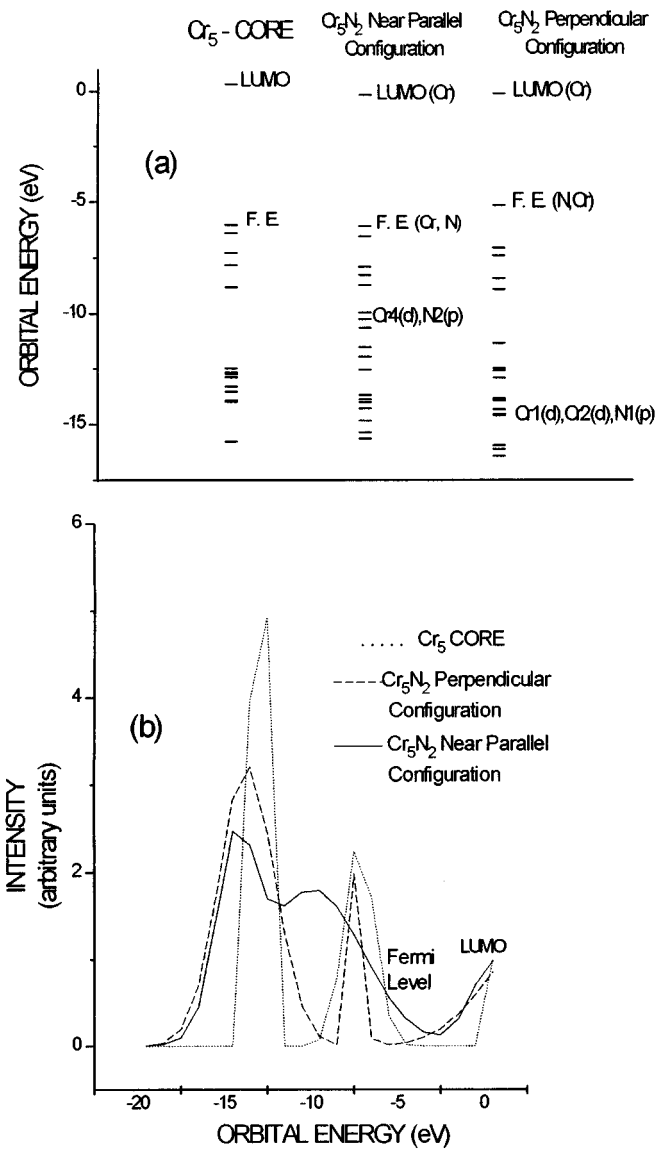

FIG. 3. (a) Orbital SCF energies for the bare cluster as well as the perpendicular and near parallel configurations (F.E. is the HOMO or Fermi energy). (b) Density of states for the bare cluster as well as the perpendicular and near-parallel configurations.

The Cr4-N2 natural bond orbital is also mostly a N2 orbital (6% s, 94% p) with Cr (6% s, 46% p, 46% d) participation.

Further investigation of the adsorbed N_2-chromium surface bonding in the nearly parallel configuration indicates that the Cr2-N2 and Cr4-N2 bonding orbitals have $\mathrm{Cr2}(d(\pi))$, $\mathrm{Cr2}(d(\sigma))$ and $\mathrm{N2}(p(\sigma))$ and $\mathrm{N2}(p(\pi))$ components and can thus have both π and σ contributions. Analysis of the largest bond hybrid coefficients indicate that for both the Cr2-N2 and Cr4-N2 bond orbitals, π interactions should be dominant, in agreement with our previous analysis.

Analysis of the density of states obtained by transforming the discrete energy levels using Gaussian distributions for the bare cluster as well as the perpendicular and parallel configurations indicates that the major changes in the density of states occurs in the parallel configurations. In these configurations the spacing of the energy levels diminishes and the density-of-states is less peaked—tending more towards

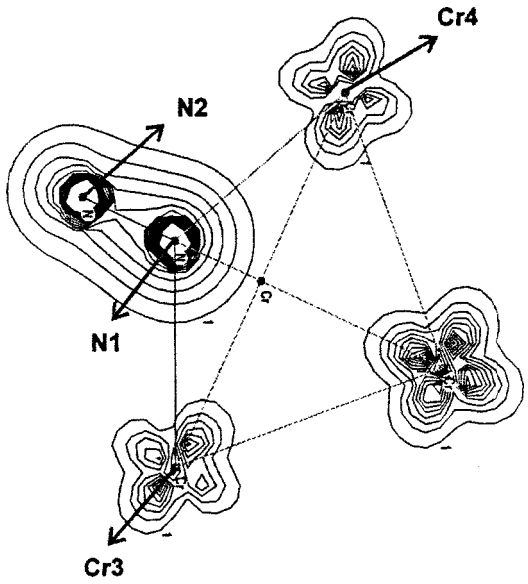

FIG. 4. Charge-density overlap plot for the perpendicular configuration in the N1, N2, Cr3, Cr4 plane.

bands—and is higher at the Fermi level. The well-separated peaks observed in the bare cluster and the perpendicular configurations are not so clearly defined in the near-parallel configuration. On the other hand, we have high density of states near the HOMO and LUMO in both parallel and perpendicular configurations. The enhanced mixing of N and Cr orbital components in the near-parallel configuration partially smears out the density of states, which is more clearly separated in the bare cluster and perpendicular state, which could explain some of the difficulties in analyzing much of the experimental photoelectron valence spectra.

In Figs. 4–8 we show the charge densities and contour plots for the perpendicular and near-parallel configurations. Figure 4 shows the charge-density overlap plot (perpendicular configuration) in the N1, N2, Cr3, Cr4 plane indicating negligible molecular interaction between the N atoms and the Cr surface atoms, as expected, due to the large interatomic distances. Figure 5 shows the charge-density overlap

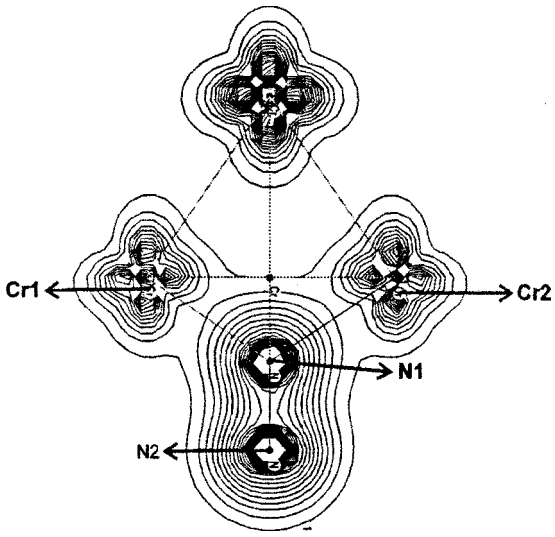

FIG. 5. Charge-density overlap plot of the perpendicular configuration in the N1, N2, Cr1, Cr2 plane.

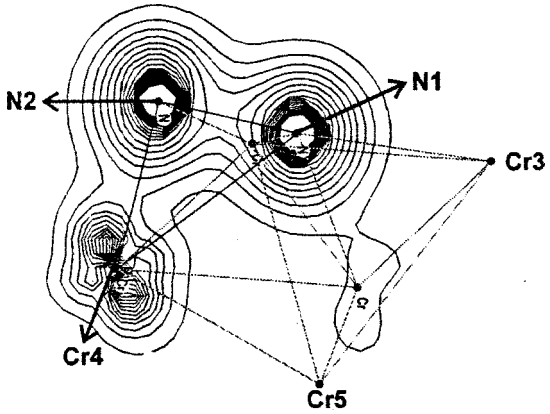

FIG. 6. Charge-density overlap plot of the near parallel configuration in the N1, N2, Cr4, Cr3 plane.

plot (perpendicular configuration) in the N1, N2, Cr1, Cr2 plane indicating molecular-orbital interaction between the nearest N1 nitrogen atom and the Cr surface (Cr1,Cr2) atoms, as expected, due to the smaller surface chromium-nitrogen distances (Fig. 1). Figure 6 shows the charge-density overlap (near-parallel configuration) in the N1, N2, Cr3, Cr4 plane indicating strong molecular interaction between the nearest nitrogen (N2) atom and Cr4 surface chromium atom as compared to, for example, the Cr3-N2 molecular-orbital interaction. We note that the N2-Cr4 molecular orbitals are also better oriented/aligned for enhanced molecular-orbital interaction. Figure 7 shows an orbital contour (below the Fermi level), in the near-parallel configuration, indicating the molecular-orbital interaction between Cr4 and N2, which has inclined from its distant perpendicular position to a closer more favorable aligned position for molecular-orbital interaction. Figure 8 shows an orbital contour plot, in the near-parallel configuration, indicating the molecular-orbital interaction between N1 and Cr1. There is a similar interaction in the perpendicular configuration since the N1 and Cr1 distance and alignment is not significantly modified. Also in this near-parallel configuration there is no

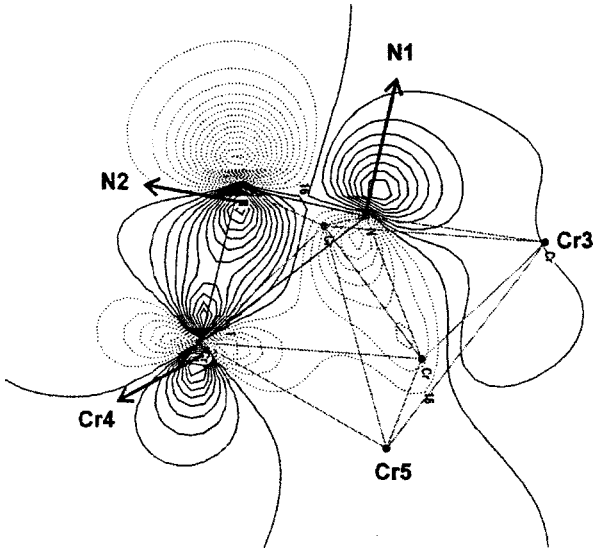

FIG. 7. Orbital contour plot indicating Cr4-N2 molecular-orbital interaction.

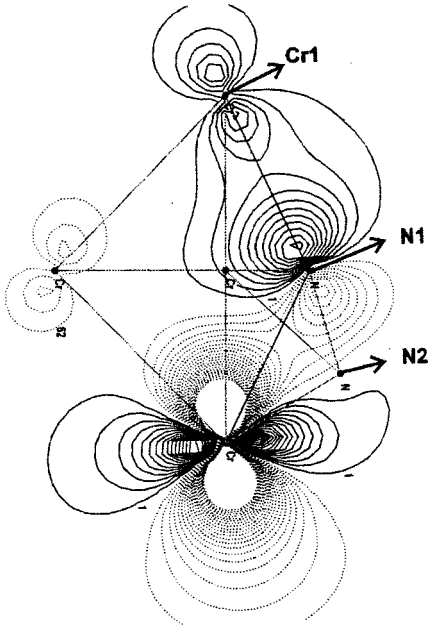

FIG. 8. Orbital contour plot indicating Cr1-N1 molecular-orbital interaction.

molecular-orbital interaction between N2 and Cr1 due to the large interatomic distance and absence of orbital alignment.

IV. CATALYSIS MODEL

In contrast to more complex, computationally expensive and conventional calculations of two- and three-dimensional reaction trajectories we propose a simple general model (Fig. 9) for the mechanism of dissociation of N_2 on transition-metal surfaces. It is a process of electron transfer—M(metal)$\rightarrow N_2$ and $N_2\rightarrow$metal via resonant states in analogy with Pauling's schematic model.[50] It is used to explain the motion of a negative charge (electron) through a metal as the covalent bonds resonate from one position to another whereas in the presence of an applied electromagnetic field the electrons tend to move in the appropriate direction from atom to atom by a succession of shifts by single bonds.

According to Pauling,[50] unsynchronized resonance requires that the atom receiving a bond (M^+ or M) have an orbital available for its reception (occupied in M^-). It is the existence of this orbital—the metallic orbital—in addition to the orbitals required for occupancy by unshared electron pairs and bonding electrons, by all or many of the atoms in a condensed phase, that permits the unsynchronized resonance of covalent bonds that gives rise to metallic properties. The back donation (charge transfer) from surface Cr atoms to the adsorbed N_2 of ~ 1 electron previously discussed would

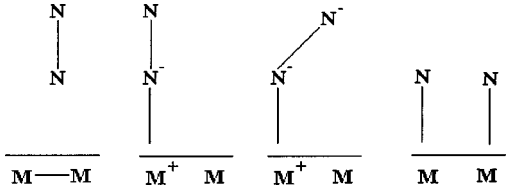

FIG. 9. Model for catalytic dissociation of N_2 on transition-metal surfaces.

contribute to creating the M^+, M^-, M states required for the unsynchronized resonance model for N_2 heterogeneously catalyzed dissociation on transition-metal surfaces. Our model also indicates the formation of the covalent bonds required for the motion of negative charges through the resonant states described above leading to dissociation of N_2 on the metal surface as the charge returns to the surface restoring its electrical neutrality.

In the first step of our model (Fig. 9) the M-M bond (where M designates surface transition-metal atom) is transferred to an antibonding orbital of N_2 which becomes a Lewis acid after receiving electrons from the metal. The surface must have available, however, electrons for this back donation. The inclination of the molecule diminishes the strength of the N—N bond leading to another phase where the electron returns to the surface thereby restoring the electrical neutrality of the catalyst. When N_2 inclines to the parallel position (Fig. 2), N1 is slightly shifted from its centrosymmetric position ~ 0.04 Å along the short axis. The reduction of symmetry is often related to the increase of the activity of the process due to a lifting of degeneracy or an increase of entropy. A detailed analysis of the experimental energetic shifts of the ionic state of the adsorbed molecule with respect to the gas phase indicates a nonsymmetric coordination site (with respect to the internuclear axis) of N_2 in the α phase.[26] With the inclination of the molecule, which as previously discussed, results in a more favorable configuration, there is an increase of negative charge on the N2 atom, the one nearest the surface having a formal positive charge. Analysis of relative energies versus inclination angle, indicates a small potential barrier at approximately 30° from the perpendicular axis to the surface. We have previously used a similar model to describe successfully the dissociation of CO on $3d$ transition-metal surfaces.[1–4] This potential barrier between the vertical and horizontal orientations is small (0.04 eV) and indicates that horizontal orientations are strongly favored, in agreement with experiment.

V. CONCLUSIONS

The interaction of N_2 with the Cr (110) surface yields useful insight regarding the mechanism of adsorption of diatomic molecules on $3d$ metal surfaces. We have proposed a model to explain the dissociation of N_2 by considering that the atoms of the surface participate in the unsynchronized resonating valence bond mechanism involving atoms of the molecule and the surface based on the closed cycle of surface→molecule, followed by molecule→surface charge transfer, with an intermediate state, with a large charge transfer, in which the molecule is inclined to the surface. Our results of Mulliken overlap population analysis, N-N distances, stretching frequencies, natural bond orbital populations, density of states, orbital energies, charge-density distribution, and orbital contours confirms the existence of the tilted molecular state, which is identified as the precursor state of the dissociation.

ACKNOWLEDGMENTS

A.C.P. and C.A.T. acknowledge financial assistance from CNPQ (Brasil). A.C.P. also thanks Finep (Brasil) for support. T.C.G. acknowledges financial assistance from CAPes. W.A.L. was supported in part by the Director, Office of Energy Research, Office of Basic Energy Sciences Chemical Sciences Division of the U. S. Department of Energy under Contract No. DE-AC03-76SF00098.

*Permanent address: Departamento de Desenho e Tecnologia, Universidade do Estado de Bahia, Salvador, Bahia, Brazil.

[1] A. C. Pavão, M. Braga, C. A. Taft, B. L. Hammond, and W. A. Lester, Jr., Phys. Rev. B **43**, 6962 (1991), and references therein.
[2] A. C. Pavão, M. Braga, W. A. Lester, Jr., B. L. Hammond, and C. A. Taft, Phys. Rev. B **44**, 1910 (1991).
[3] A. C. Pavão, M. M. Soto, W. A. Lester, Jr., S. K. Lie, B. L. Hammond, and C. A. Taft, Phys. Rev. B **50**, 1868 (1994).
[4] A. C. Pavao, B. L. Hammond, M. M. Soto, W. A. Lester, Jr., and C. A. Taft, Surf. Sci. **323**, 340 (1955).
[5] G. Blyholder, J. Phys. Chem. **68**, 2772 (1964).
[6] N. D. Shinn and T. E. Madey, J. Chem. Phys. **83**, 15 928 (1985); Phys. Rev. B **33**, 1464 (1986); N. D. Shinn, *ibid.* **38**, 12 248 (1988); **41**, 9771 (1990); C. Benndorf, B. Kruger, and F. Thieme, Surf. Sci. **163**, L675 (1985).
[7] H. Ueba, Surf. Sci. **169**, 153 (1986).
[8] K. Horn, J. Dinardo, W. Eberhard, and E. W. Plummer, Surf. Sci. **118**, 465 (1982).
[9] B. E. Nieuwenhuys, Surf. Sci. **105**, 505 (1981).
[10] P. S. Bagus, C. R. Brundle, K. Hermman, and D. Menzel, J. Electron Spectrosc. Relat. Phenom. **20**, 253 (1980).
[11] P. A. Dowben, Y. Sakisaka, and T. N. Rhodin, Surf. Sci. **147**, 89 (1984).
[12] D. Heskett, E. W. Plummer, R. A. Depaola, W. Eberhardt, F. M. Hoffmann, and H. R. Moser, Surf. Sci. **164**, 490 (1985).
[13] E. Umbach, Solid State Commun. **51**, 365 (1984).
[14] W. Ho, R. F. Willis, and E. W. Plummer, Surf. Sci. **95**, 171 (1980).
[15] G. Hasse and M. Asscher, Surf. Sci. **191**, 75 (1987).
[16] D. E. Ibbotson, T. S. Wittrig, and W. H. Weinberg, Surf. Sci. **110**, 313 (1981).
[17] R. A. Depaola and F. M. Hoffmann, Chem. Phys. Lett. **128**, 343 (1986).
[18] R.-H. Zhou, D.-H. Shi, and P.-L. Cao, J. Phys. Condens. Matter **4**, 2429 (1992).
[19] Y. Wu and P.-L. Cao, Surf. Sci. **203**, L651 (1988); **179**, L26 (1987).
[20] J. Stöhr and R. Jaeger, Phys. Rev. B **26**, 4111 (1982).
[21] W. F. Egelhoff, Jr., Surf. Sci. **141**, L324 (1984).
[22] D. Tomanek and K. H. Bennemann, Phys. Rev. B **31**, 2488 (1985).
[23] W. Ho, R. F. Willis, and E. W. Plummer, Surf. Sci. **95**, 171 (1980).
[24] G. Ertl and J. Kuppers, Phys. Rev. Lett. **53**, 850 (1984).
[25] M. Grunze, M. Golze, W. Hirschwald, H. J. Freund, H. Pulm, U. L. Seip, N. C. Tsai, G. Ertl, and J. Kuppers, Phys. Rev. Lett. **53**, 850 (1984).
[26] H. J. Freund, B. Bartos, R. P. Messmer, M. Grunze, H. Kuhlenbeck, and M. Neumann, Surf. Sci. **185**, 187 (1987).
[27] Y. Fukuda and M. Nagosgi, Surf. Sci. **203**, L651 (1988).
[28] N. D. Shinn, Phys. Rev. B **41**, 9771 (1990).
[29] E. W. Plummer, C. T. Chem, W. K. Ford, W. Eberhardt, R. P.

Messmerand, and H. J. Freund, Surf. Sci. **158**, 58 (1985).
[30] H. Ibach and D. L. Mill, *Electron Energy-Loss Spectroscopy and Surface Vibration* (Academic, New York, 1982).
[31] H. J. Freund, W. Eberhardt, D. Heskett, and E. W. Plummer, Phys. Rev. Lett. **50**, 768 (1983).
[32] D. R. Norton, R. L. Tapping, and J. W. Goodale, Surf. Sci. **72**, 33 (1978).
[33] K. Hermann and P. S. Bagus, Solid State Commun. **38**, 1257 (1981).
[34] D. Heskett, E. W. Plummer, and R. P. Messmer, Surf. Sci. **139**, 558 (1984).
[35] G. D. Mahan and A. A. Lucas, J. Chem. Phys. **168**, 1344 (1978).
[36] F. Bozso, G. Ertl, M. Grunze, and M. Wiss, J. Catal. **49**, 18 (1977).
[37] N. D. Spencer, R. C. Schoonmaker, and G. A. Somorjai, J. Catal. **74**, 129 (1982).
[38] M. C. Tsai, U. Seip, I. C. Bassignana, J. Küppers and G. Ertl, Surf. Sci. **155**, 387 (1985).
[39] L. J. Whitman, C. E. Bartosch, and W. Ho, J. Chem. Phys. **85**, 3788 (1986).
[40] P. A. Dowben, A. Miller, H.-J. Ruppender, and M. Grunze, Surf. Sci. **193**, 336 (1988).
[41] P. A. Dowben, H.-J. Ruppender, and M. Grunze, Surf. Sci. **254**, L482 (1991).
[42] M. Sinder, D. Fuks, and J. Pelleg, Phys. Rev. B **50**, 2775 (1994).
[43] E. O. F. Zdansky, A. Nilsson, H. Tillborg, O. Bjorneholm, and N. Martensson, Phys. Rev. B **48**, 2632 (1993).
[44] A. Sandell, O. Bjorneholm, A. Nilsson, E. O. F. Zdansky, H. Tillborg, J. N. Andersen, and N. Martensson, Phys. Rev. Lett. **70**, 2000 (1993).
[45] J. Zhao, X. Chen, and G. Wang, Phys. Rev. B **20**, 424 (1994).
[46] B. Piveteau, D. Slpanjaard, and M. C. Desjouqueres, Phys. Rev. B **49**, 8402 (1994).
[47] J. E. Ortega, F. J. Himpsel, R. Haight, and D. R. Peale, Phys. Rev. B **49**, 859 (1994).
[48] O. Bjormehjolm, H. L. Tillborg, A. Nisson, and N. Martensson, Phys. Rev. Lett. **19**, 2551 (1994).
[49] O. Bjorneholm, A. Nilsson, E. O. F. Zdansky, A. Sandell, and H. Tillborg, Phys. Rev. B **47**, 2308 (1993).
[50] L. Pauling, Solid State Chem. **54**, 297 (1984).
[51] M. J. Frisch, G. W. Trucks, M. Head-Gordon, P. M. W. Gill, M. W. Wong, J. B. Foresman, B. G. Johnson, H. B. Schlegel, M. A. Robb, E. S. Repllogle, R. Gomperts, J. L. Andres, K. Rachavachari, J. S. Binleyh, C. Gonzalez, R. L. Martin, D. J. Fox, D. J. Defrees, J. Baker, J. J. P. Stewart, and J. A. Pople, *Gaussian 92*, (Gaussian, Inc., Pittsburgh 1992).
[52] J. Hay and W. R. Wadt, J. Chem. Phys. **82**, 270 (1985).
[53] A. E. Reed, R. B. Weinstock, and F. Weinhold, J. Chem. Phys. **83**, 735 (1985).
[54] R. F. W. Bader, *Atoms in Molecules: A Quantum Theory* (Oxford University Press, Oxford, 1990); K. B. Wiberg and P. R. Rablen, J. Comput. Chem. **14**, 1504 (1993); *Exploring Chemistry with Electronic Structure Methods*, edited by J. B. Foresman and A. Frisch (Gaussian, Inc., Pittsburgh, 1996); R. S. Mulliken, J. Chem. Phys. **23**, 1833 (1955); L. Pauling, *The Nature of the Chemical Bond* (Cornell University Press, Ithaca, 1960).